

Systematic Discovery of Rab GTPases with Synaptic Functions in *Drosophila*

Chih-Chiang Chan,^{1,11} Shane Scoggin,^{2,11} Dong Wang,¹
Smita Cherry,¹ Todd Dembo,^{1,7} Ben Greenberg,^{1,8}
Eugene Jennifer Jin,¹ Cansu Kuey,^{1,9} Antonio Lopez,³
Sunil Q. Mehta,^{3,10} Theodore J. Perkins,⁵
Marko Brankatschk,⁶ Adrian Rothenfluh,³
Michael Buszczak,^{2,*} and P. Robin Hiesinger^{1,4,*}

¹Department of Physiology

²Department of Molecular Biology

³Department of Psychiatry

⁴Green Center for Systems Biology

UT Southwestern Medical Center, Dallas, TX 75390, USA

⁵Ottawa Hospital Research Institute, Ottawa,

ON K1Y 4E9, Canada

⁶Max Planck Institute for Cell Biology,
01307 Dresden, Germany

Summary

Background: Neurons require highly specialized intracellular membrane trafficking, especially at synapses. Rab GTPases are considered master regulators of membrane trafficking in all cells, and only very few Rabs have known neuron-specific functions. Here, we present the first systematic characterization of neuronal expression, subcellular localization, and function of Rab GTPases in an organism with a brain.

Results: We report the surprising discovery that half of all *Drosophila* Rabs function specifically or predominantly in distinct subsets of neurons in the brain. Furthermore, functional profiling of the GTP/GDP-bound states reveals that these neuronal Rabs are almost exclusively active at synapses and the majority of these synaptic Rabs specifically mark synaptic recycling endosomal compartments. Our profiling strategy is based on Gal4 knockins in large genomic fragments that are additionally designed to generate mutants by end-out homologous recombination. We generated 36 large genomic targeting vectors and transgenic *rab*-Gal4 fly strains for 25 *rab* genes. Proof-of-principle knockout of the synaptic *rab27* reveals a sleep phenotype that matches its cell-specific expression.

Conclusions: Our findings suggest that up to half of all *Drosophila* Rabs exert specialized synaptic functions. The tools presented here allow systematic functional studies of these Rabs and provide a method that is applicable to any large gene family in *Drosophila*.

Introduction

Rab GTPases were first described in 1987 when Touchot and colleagues isolated four family members from a rat brain cDNA library and consequently named them “*rab*” for “*ras* gene from rat brain” [1]. Subsequent work over the last 24 years has firmly established *rab* GTPases as key regulators of membrane organization and intracellular membrane trafficking in all eukaryotic cells [2–5]. The majority of Rab GTPases are thought to serve ubiquitous cell biological functions.

Rab proteins cycle between active and inactive states. In response to signal stimuli, guanine nucleotide exchange factors (GEFs) interact with Rab GTPases and trigger their binding to GTP. In the GTP-bound active form, each Rab interacts with a different complex of proteins (effectors) to facilitate the delivery of transport vesicles to different acceptor membranes [6, 7]. GTPase-activating proteins (GAPs) work in the opposite direction and accelerate Rab GTP hydrolysis, typically rendering the subsequently GDP-bound Rab proteins inactive.

Neurons have specialized demands on membrane trafficking both during development (wiring-specific extensive arborizations) and function (neurotransmitter release). The importance of Rab function in the nervous system is highlighted by the observation that mutations in *rab* genes and their regulators cause several hereditary and neurological diseases including Griscelli syndrome (Rab27), Charcot-Marie-Tooth type 2B disease (Rab7), Warburg Micro syndrome (a GTPase activating protein for Rab3), X-linked mental retardation (RabGDI—a Rab GTP dissociation inhibitor), and Hermansky-Pudlak syndrome (a Rab geranylgeranyl transferase) [8–11]. Recently, Rab8-dependent trafficking was identified as a key mechanism underlying Bardet-Biedl syndrome, which causes retinopathy and blindness [12]. In *Drosophila*, Rab11 is required for post-Golgi trafficking of rhodopsin [13] and guidance receptors during brain wiring [14]. Lastly, active zone assembly at synapses requires Rab3 [15]. Although these examples underscore the importance of Rab-dependent trafficking in neurons, comprehensive profiling of *rab* GTPase function in a brain at cellular and subcellular resolutions in vivo has not been attempted.

Drosophila is ideally suited for the systematic study of *rab* GTPases in the nervous system. There are 31 potential *rab* or *rab*-related genes in the fly genome of which at least six have no clear vertebrate ortholog [16]. Twenty-three *rab* genes have direct orthologs in human that are at least 50% identical at the protein level (see also Figure S4 available online). Hence, Rab proteins in *Drosophila* exhibit high evolutionary conservation and low redundancy compared to over 70 *rabs* in vertebrates [16]. For example, the best-characterized neuronal *rab* GTPase, *rab3*, exists as four partially redundant genes in vertebrates but as a single gene in *Drosophila*. Yet, clear orthologs exist and serve as gold standard markers for many intracellular compartments across species. These include Rab1 for the endoplasmic reticulum, Rab5 for early endosomes, Rab6 for the Golgi, Rab7 for multivesicular bodies, and Rab11 for recycling endosomal compartments [7, 17, 18]. Recently developed tools combined with established

⁷Present address: University of California San Francisco, San Francisco, CA 94143, USA

⁸Present address: University of California San Diego, La Jolla, CA 92093, USA

⁹Present address: Bilkent University, 06800 Bilkent, Ankara, Turkey

¹⁰Present address: University of California Los Angeles, Los Angeles, CA 90095, USA

¹¹These authors contributed equally to this work

*Correspondence: michael.buszczak@utsouthwestern.edu (M.B.), robin.hiesinger@utsouthwestern.edu (P.R.H.)

Drosophila genetics allow for the systematic characterization of this complete gene family in vivo [16, 19]. We generated ends-out homologous recombination competent targeting vectors of typically >50 kb for 25 conserved *rab* loci using a bacterial artificial chromosome (BAC)-mediated recombining. Within these vectors we replaced the *rab* genes with the yeast transcription factor Gal4, yielding “Gal4 drivers,” and inserted them at a predefined landing site within the genome prior to labor-intensive homologous recombination experiments. This enabled us to perform a systematic profiling of the cellular and subcellular expression of Rab GTPases in *Drosophila* in combination with an existing collection of UAS-YFP-Rabs transgenic fly lines. Our profiling reveals that half of all *rab* GTPases are neuron-specific or strongly enriched in varying and specific subsets of neurons in the brain and that all neuronal *rabs* encode synaptic proteins. Finally, we perform a proof-of-principle knockout screen for the neuron-specific *rab27* gene and describe a specific behavioral sleep defect for the *rab27* null mutant that matches its cell-specific expression.

Results

Generation of 36 *rab*-Gal4 Knockin Vectors and Transgenic Fly Strains for Ends-Out Homologous Recombination Using BAC Recombineering and PhiC31 Transgenesis

In order to genetically characterize and manipulate all members of the *rab* gene family in parallel, we devised a modification to P[acman] technology by incorporating an optimized ends-out homologous recombination cassette [20], thereby generating the P[acman]-KO vector (Figure 1A). Using recombineering [21], we generated 41 P[acman]-KO targeting vectors of typically more than 50 kb, centered on individual *rab* loci. A key advantage of using large genomic fragments is that they are predicted to contain all regulatory elements; fully functional genomic rescue fragments in *Drosophila* are traditionally between 5–10 kb. In these large genomic regions, we used a positively marked knockin cassette (Figure 1B) to replace *rab* genes with the yeast transcription factor Gal4, yielding Gal4 driver lines. These Gal4 lines are functional after integration in a landing site and can be utilized for expression and functional profiling prior to labor-intensive homologous recombination experiments. All technical details and protocols are available in the Supplemental Experimental Procedures.

We designed targeting vectors for two types of knockins: first, we replaced complete open reading frames (ORFs) with Gal4 for 27 *rab* loci (red arrows and primer pairs in Figure 1C and Figure S1). These targeting vectors are designed for the generation of unequivocal null mutants and are referred to as “ORF knockins.” For two additional loci (*rab26* and *rab32*) we chose to only replace short coding regions of the first exons because of the large size of the genomic loci (Figure S1). Second, we replaced only the short coding regions starting with the ATG to the end of the ATG-containing exon for 12 *rab* loci in cases where the ORF knockins delete potential regulatory sequences (blue arrows and primer pairs in Figure 1C and Figure S1). These Gal4 knockins are designed to ensure that the resulting lines express Gal4 in the endogenous gene expression pattern. We refer to these as “ATG knockins.” The generation of these 12 alternative targeting vectors was straightforward, because only one round of recombineering is required to replace a different sequence in the targeting vectors that already contain the genomic DNA, highlighting the efficiency of the recombineering approach. Figure 1C

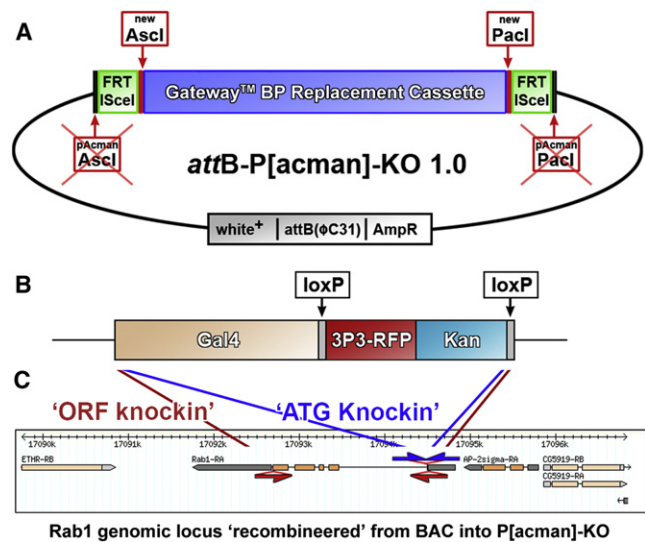


Figure 1. Design of P[acman]-KO: Combining BAC Recombineering, PhiC31 transgenesis, and Ends-Out Homologous Recombination

(A) Vector design. First, a [Frt, ISce1] cassette was inserted into the Ascl and Pacl sites of attB-P[acman]-Ap^R to add mobilization capability for endogenous targeting. Second, a Gateway™ cassette for bacteriophage λ-mediated BP recombination was introduced with new Ascl and Pacl sites. Hence, homology arm cassettes can either be integrated using Ascl, Pacl conventional cloning, or by including Gateway™ attB sites into the primers used to create such cassettes. See Supplemental Experimental Procedures for more details. All other features of the vector are described in [31].

(B) Design of the Gal4 knockin cassette. This 6.7 kb cassette is adapted for desired loci by including gene-specific 100 bp homology arms in the primers used to amplify the cassette. Note that optimized PCR conditions are identical for any primer pair (see Supplemental Experimental Procedures). The floxed 3xP3-RFP, Kan cassette serves for selection during bacterial recombineering cloning (Kan) and positive selection of the targeting cassette in a homologous recombination experiment in vivo in the fly (3xP3-RFP) and can be removed in transgenic or gene-targeted flies easily by crossing to available Cre strains.

(C) Strategies for open reading frame (ORF) and ATG knockins. The Gal4 knockin cassette replaces the complete open reading frame in ORF knockins, whereas in ATG knockins only the start codon and the remaining part of the start-codon containing exon are replaced. Note that in both cases the ATG of Gal4 replaces the ATG of the *rab* gene.

shows the “ORF knockin” and “ATG knockin” for the *rab1* locus; all loci are shown in Figure S1. In most cases, the Gal4 cassette was knocked into a genomic fragment of 40 kb, with few exceptions where cloning of the large region proved difficult (*rab5*: 30 kb; *rab18*, *rab19*: 20 kb). In total, we generated 41 targeting vectors for the generation of transgenic flies to create Gal4 driver lines under the endogenous regulatory elements of 29 *rab* loci (Figure S1).

Recovery of transgenic flies for the large vectors (>55 kb) was challenging with typically less than one transformant in 10,000 progeny; however, recent efforts show that this can be substantially improved [22, 23]. For five genomic constructs, we could not obtain transgenics after injection of more than 1,500 embryos (“ORF knockins” of *rab4*, *rab30*, *rab40*, *rabX5*, and *rabX6*). We obtained transgenic flies for 24 “ORF knockins” and all 12 “ATG knockins” (including *rab4*). In total, we obtained 36 transgenic fly strains for 25 *rab* loci.

To determine the expression patterns of these *rab* genes, we crossed the *rab*-Gal4 lines to UAS-CD8-GFP and analyzed the brains, eye discs, wing discs, leg discs, and salivary glands of *rab*-Gal4 > UAS-CD8-GFP third-instar larvae and obtained

confocal high-resolution 3D data sets in duplicate or triplicate for each line and each tissue. Antibodies or GFP tags in the genomic loci exist for some *rabs* providing independent verification of the fidelity of our Gal4 lines (Figures S2A–S2H). In addition, we performed rescue experiments for existing mutants or knockouts generated with the technique presented here to verify the accuracy of the Gal4 lines including *rab3* and *rab6* (Figures S2I–S2N) and the *rab27* knockout presented below. By these various methods we verified *rab2*, *rab3*, *rab5*, *rab6*, *rab7*, *rab11*, and *rab27*, and in no case did we find evidence for significant expression differences between the *rab*-Gal4 knockins and endogenous *rabs*. For the detailed characterizations in the following sections, we selected the 12 ATG knockins, additional ATG/exon 1 knockins for *rab26* and *rab32*, and ORF knockins for the remaining nine *rab* loci.

Cellular Expression Profiling Reveals that Half of All *rabs* Are Neuron-Specific or Strongly Neuron-Enriched with Highly Variable Expression Patterns in the Brain

The selected *rab* lines exhibit a surprising variety of expression patterns with a strong bias for the nervous system (Figure 2). Specifically, we identified six lines with expression exclusively in neurons and possibly glia in the larval brain (*rab3*, *rab19*, *rab26*, *rab27*, *rab32*, and *rabX4*). Furthermore, *rab9*-Gal4, *rab21*-Gal4, *rab23*-Gal4, and *rabX1*-Gal4 exhibit expression exclusive to neurons, glia, and salivary glands (a nonneuronal secretory tissue). *rab4*-Gal4, *rab7*-Gal4, *rab10*-Gal4, *rab14*-Gal4, and *rab39*-Gal4 exhibit their strongest expression in neurons but also diverse patterns of expression in other tissues. Finally, we found ubiquitous expression patterns, albeit with different expression levels in different tissues and neurons, for only eight lines (*rab1*, *rab2*, *rab5*, *rab6*, *rab8*, *rab11*, *rab18*, and *rab35*). Hence, half of the *rab*-Gal4 lines analyzed here exhibit neuron-specific or strongly neuron-enriched expression. Neuronal Rabs are present in all major branches of the phylogenetic tree, and protein similarity does not correlate with neuronal expression (Figure S3A).

Of the ten *rab*-Gal4 lines that exclusively express in neurons, glia and salivary glands only *rab3*-Gal4 and *rabX4*-Gal4 exhibit broad neural expression (Figure 2). In contrast, all other lines express in surprisingly specific and varying subsets of neurons. The highest expression overlap is in the ventral ganglion, where the motor neurons that innervate the body wall musculature reside; the highest diversity of expression patterns is apparent in the functioning and developing central brain. Developing photoreceptor neurons only show strong and neuron-specific expression in the eye discs of *rab3*-Gal4, *rabX4*-Gal4, *rab9*-Gal4, *rab14*-Gal4 (with some non-neuronal cells), and, surprisingly, *rab7*-Gal4, which is not neuron-specific in other tissues and later during development expresses more ubiquitously. Taken together, our findings suggest that *rab* GTPases have highly diverse expression patterns in active neurons in particular.

All *rab* GTPases Are Strongly Expressed in Functional Neurons and None Exclusively in Developing Neurons

Although all *rab*-Gal4 lines exhibit expression in at least some active neurons of the larval ventral ganglion, expression levels in the developing pupal brain (30%–40% of pupal development) vary greatly (Figure 3A). Expression in different subsets of developing neurons is apparent for all *rab*-Gal4 lines. The strongest glial driver is *rab9*-Gal4. None of the *rab*-Gal4 lines drive expression that increases during development and

decreases in the adult. The most prominent hallmark of the expression differences is the cell-type specificity, suggesting neuronal subtype-specific employment of Rab-mediated membrane trafficking during brain development.

Adult brains (1 day old) exhibit a similar variety of expression patterns (Figure 3B). Four *rabs* exhibit sparse expression patterns: *rab9*-Gal4, which is almost exclusively expressed in glia and neurons of the olfactory system, *rab19*-Gal4, which is strong in a subset of central brain neurons, *rab23*-Gal4, which is strong in the antennal lobes, and *rab27*-Gal4, which is highly restricted to few central brain neurons including Kenyon cells of the mushroom bodies. For most of the other lines, strong differences can be observed in expression levels between different neuronal cell types, suggesting differential employment in the various neuronal subtypes. Similar to pupal brain, we find no obvious adult glial expression for the Gal4 lines of the neuronal *rab3*, *rab23*, *rab26*, *rab27*, *rab32*, *rabX1*, and *rabX4*. Strong expression in mushroom bodies is apparent for an increased number of lines compared to pupal brain, including *rab1*, *rab2*, *rab3*, *rab5*, *rab6*, *rab7*, *rab8*, *rab11*, *rab14*, *rab18*, *rab27*, *rab35*, *rabX1*, and *rabX4*. Closer investigation of the high-resolution data further yields a wealth of data; e.g., lines with high level expression in mushroom bodies also exhibit high levels of expression in photoreceptors (note that photoreceptors are colabeled with the 3xP3-RFP of the knockin cassettes in Figure 3B). We conclude that *rab* GTPases exhibit highly dynamic and variable expression in the different neuronal subtypes of the developing and functional brain. However, the adult expression patterns do not change notably with age, as shown for 1 week and 3-week-old brains of eight neuronal *rabs* in Figure S4A.

All Neuronal *rabs* Encode Synaptic Proteins

Next, we investigated the subcellular localization of the different Rabs in neurons in which they are endogenously expressed by expressing YFP-tagged versions of the wild-type proteins [16]. We expect that the *rab*-Gal4 > UAS-YFP-Rab expression system recapitulates spatiotemporal expression dynamics; however, the amplification effect of the Gal4/UAS system may cause overexpression of YFP-Rab proteins compared to endogenous expression levels. Importantly, wild-type Rab proteins typically do not have overexpression phenotypes, and expression of fluorescently tagged Rab proteins is an accepted standard for the study of wild-type function in cell culture. We tested the effect of YFP-Rab overexpression in vivo in a characterized neuronal cell type by expressing all YFP-Rab proteins in photoreceptor neurons using the strong *GMR*-Gal4 driver line [24]. Indeed, none of the wild-type YFP-Rab proteins cause developmental defects based on eye morphology or photoreceptor functional defects based on electroretinogram recordings (data not shown). Similarly, no deleterious effects were observed for any UAS-YFP-Rab expression when expressed with the corresponding *rab*-Gal4 line (see below). We conclude that Gal4/UAS expression of YFP-tagged Rabs does not cause obvious developmental or functional defects. However, it has long been known that overexpression of several wild-type Rab proteins causes enlargements of the intracellular organelles they mark (e.g., [25]). Indeed, we have observed this phenomenon for several of the Rab GTPases, as presented below. The enlarged wild-type compartments provide an advantage for the profiling presented here, as size- and fluorescence-increased compartments are easier identified and colabeled with other compartment markers.

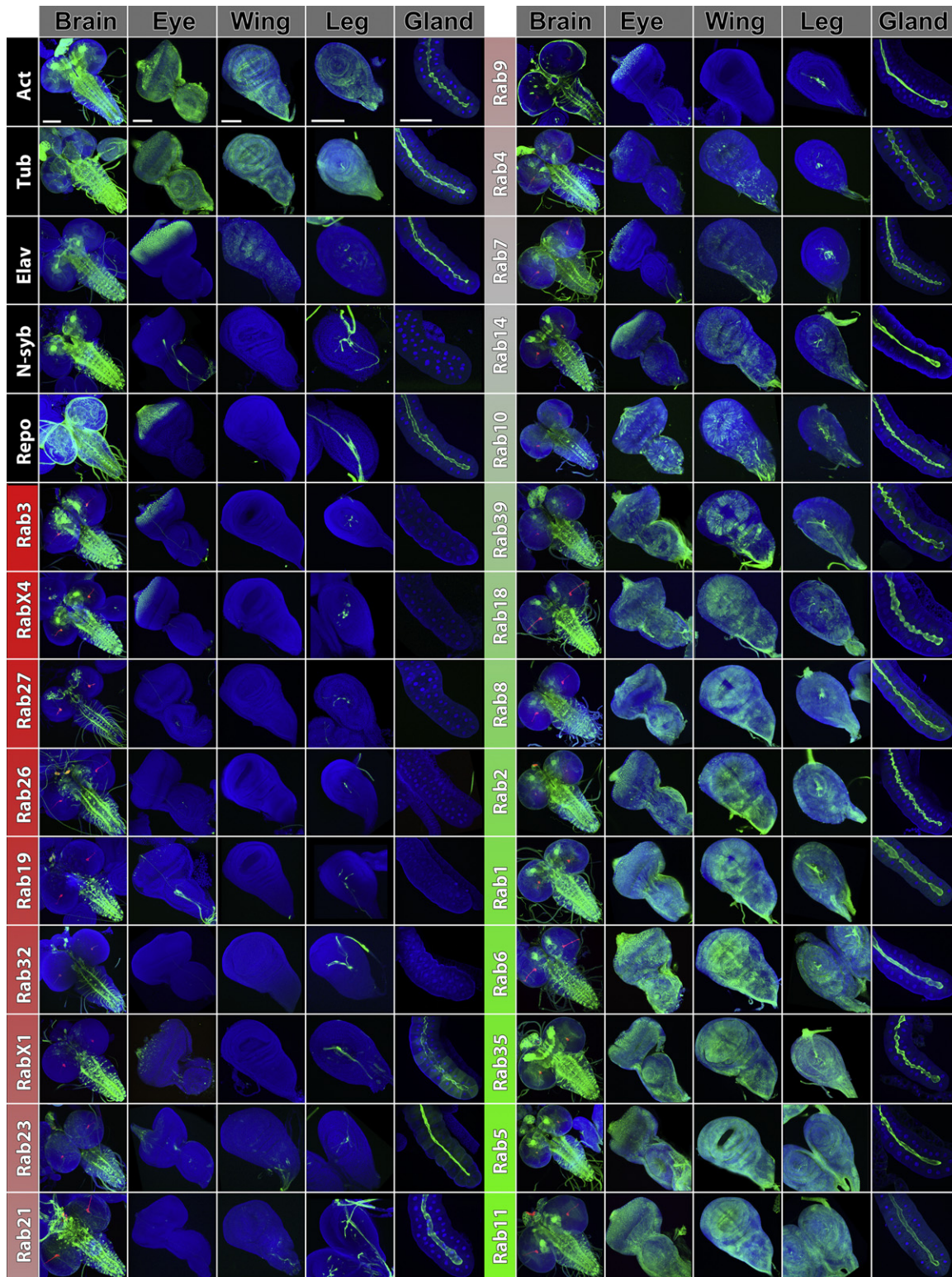


Figure 2. Systematic Expression Profiling in Larval Tissues Reveals that Half of All *rab* GTPases in *Drosophila* Are Neuron-Specific or Neuron-Enriched
Shown are the five larval tissues: brain, eye disc, wing disc, leg disc, and salivary gland (from left to right) for a total of 23 *rab*-Gal4 lines crossed to UAS-CD8-GFP (green). *Toto-3* labels nuclei (blue) and the 3xP3-RFP cassette from our knockin cassette mark the termini of the larval photoreceptor organs in the brain (red). On the top left, five control Gal4 lines are shown: *act*-Gal4 and *tub*-Gal4 (both showing ubiquitous expression), *elav*-Gal4 (showing expression in developing and functional neurons as well as low levels in some other cells), *n-syb*-Gal4 (showing panneuronal expression), and *repo*-Gal4 (showing expression in all glial cells). All *rabs* are sorted from the most neuron-specific in red (starting with *rab3* and *rabX4*), via lines with somewhat specialized patterns in gray to the most ubiquitous Gal4 driver lines in green (*rab5*-Gal4 and *rab11*-Gal4) (brain, L3 larval brain; eye, L3 eye disc; wing, L3 wing disc; leg, L3 leg disc; gland, L3 salivary gland). Scale bar for each tissue represents 100 μm .

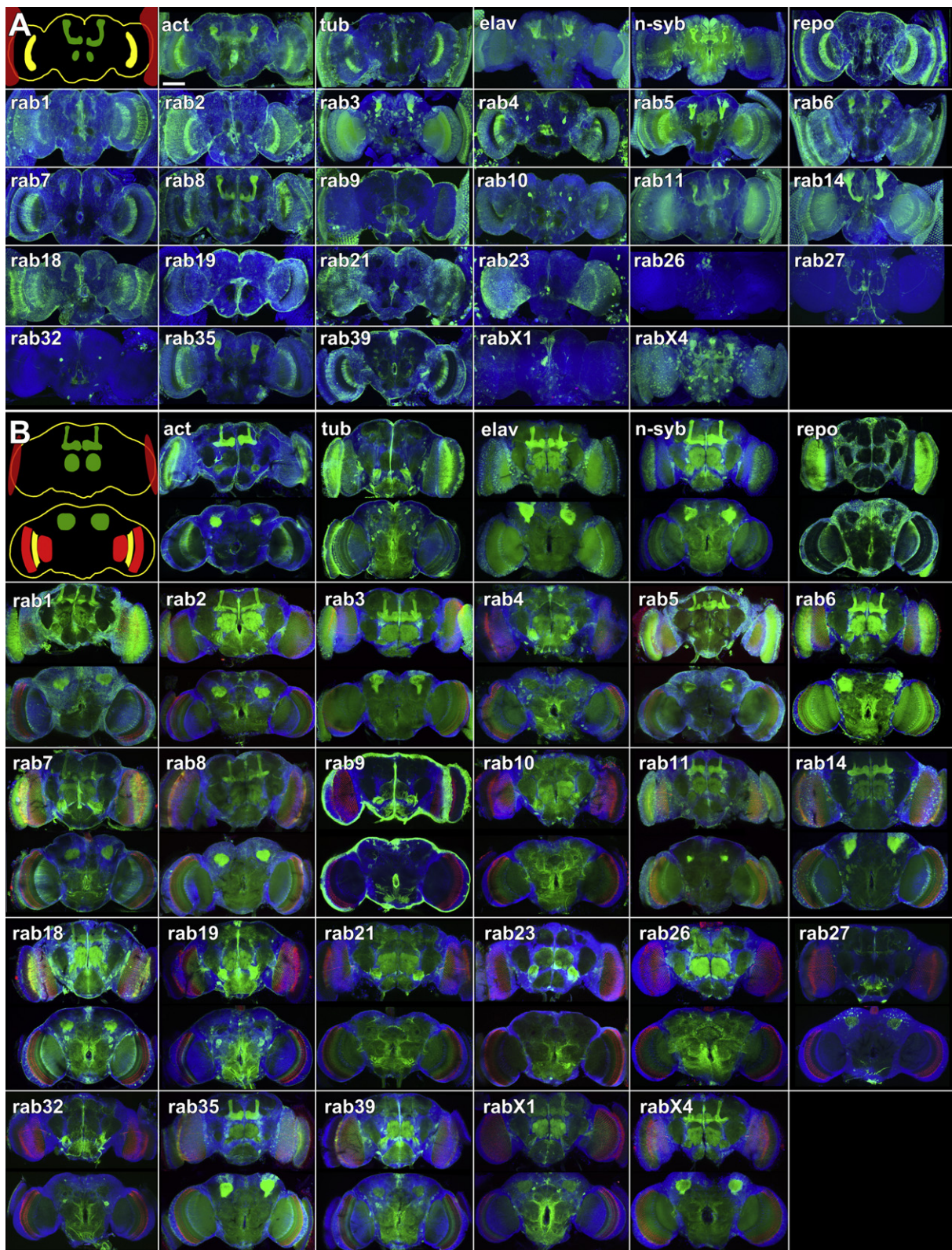


Figure 3. *rab-Gal4* Expression Patterns in the Pupal and Adult Brain

(A) Pupal brains (30%–40% pupal development). Shown are maximum projections with CD8-GFP driven by the denoted *rab-Gal4* lines (green) and nuclear labeling with Toto-3 (blue). The top left corner shows a schematic with a few prominently labeled landmark structures: the developing eyes (red), glia (yellow), and developing mushroom bodies and antennal lobes (green).

(B) Adult brains. Shown are partial maximum projections of 20 μm depth of the anterior adult brain on top and 20 μm depth of the posterior brain on the bottom. CD8-GFP is driven by the denoted *rab-Gal4* line (green), the 3xP3-RFP marker from the knockin cassette labels the photoreceptor projections

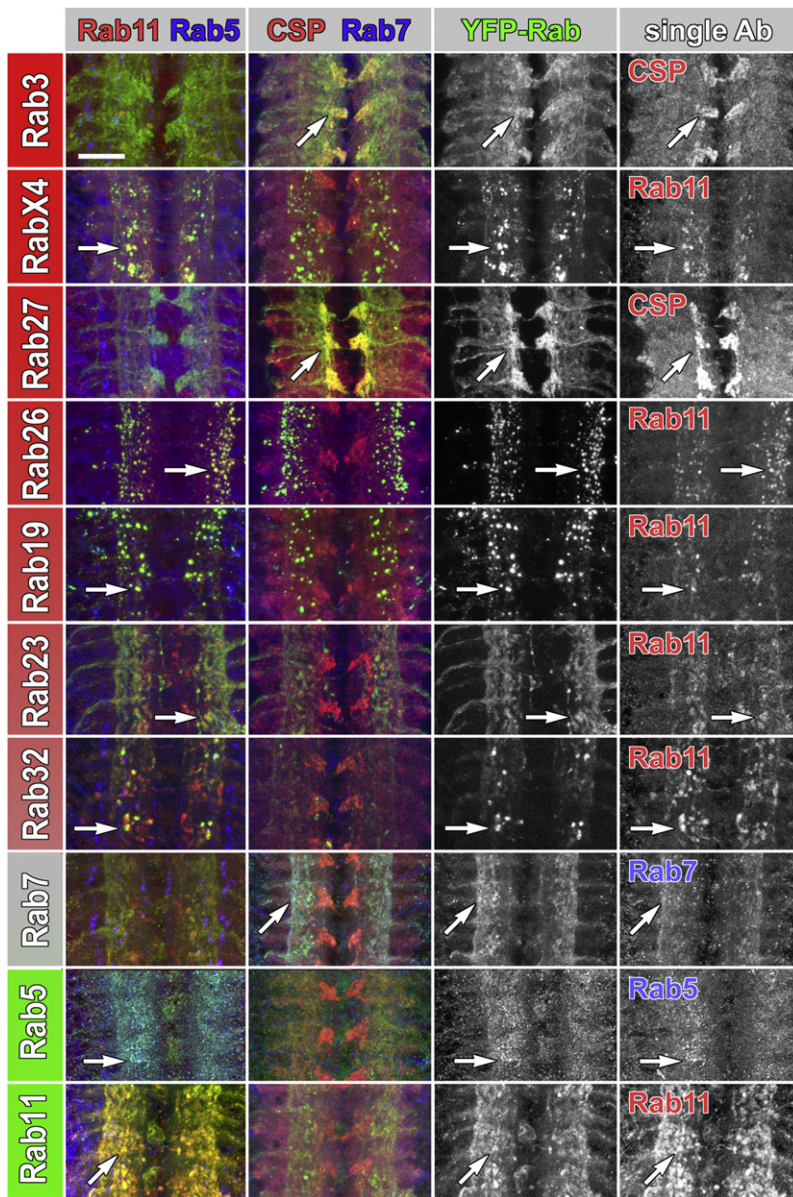


Figure 4. Subcellular Localization Profiling of YFP-Tagged Rab Proteins Expressed under Control of Their Endogenous Regulatory Elements

All neuronal *rabs* encode synaptic proteins that colocalize with recycling endosome or synaptic vesicle markers. Double immunolabelings of the posterior larval brain ventral ganglion at high resolution are shown for selected YFP-Rabs driven by their respective *rab*-Gal4 lines (green), anti-Rab11 (red, recycling endosomes), and anti-Rab5 (blue, early endosomes) labeling in the first column and anti-CSP (red, synaptic vesicles) and anti-Rab7 (blue, late endosomes) in the second column. Cell bodies are peripherally and synaptic neuropils centrally located. Single channels of the colocalizing labels are depicted in the two columns on the right. Shown are only the seven most neuron-specific lines and *rab5*, *rab7*, and *rab11* as controls; see Figure S5A for the complete dataset. Arrows point to colocalizing compartments. Scale bar for all panels represents 20 μ m.

neuron specific (Rab5, Rab7, Rab11, Rab35). Finally, only five Rab proteins exhibit mostly cell body localization, all of which are ubiquitously expressed (Rab1, Rab2, Rab14, Rab18, Rab39). Hence, all neuronal Rabs display synapse-specific or synapse-enriched localization (Figure 4; Figure S5A; Table 1). These observations suggest that approximately half of all Rab proteins not only serve neuron-specific tasks but also function to meet the demands of synapse-specific membrane trafficking.

The high-resolution confocal analysis of the synaptic region of the ventral ganglion does not reveal pre- versus postsynaptic localization. We therefore analyzed the larval neuromuscular junction (NMJ) for neuronal Rabs. As shown in Figure S6A, Rab3, RabX4, Rab26, and Rab19 exhibit clear localization inside presynaptic boutons. In contrast, Rab23 is strongly enriched on the outside of boutons, suggesting postsynaptic localization, and Rab21 is mostly localized to compartments in the muscle. Rab27, Rab32, and RabX1 are not detected at the NMJ, either because the protein is not synaptic in

We chose the posterior segments of the ventral ganglion with high commonality between the *rab* lines to study the subcellular distribution of all Rabs expressed under control of their own regulatory elements (Figure 4; complete data set in Figure S5A). Strikingly, all neuronal Rabs exhibit either synapse-specific localization (Rab3, RabX4, Rab27, Rab26, RabX1) or strongly synaptic enriched localization if some compartments are discernible also in cell bodies (Rab9, Rab19, Rab21, Rab23, Rab32) (Figure S5A). The synaptic localization is specific to the YFP-Rab proteins, because both CD8-GFP (Figure 2) and cytosolic GFP (Figure S4B) expressed using the same *rab*-Gal4 lines exhibit evenly cell body and synaptic distribution. In contrast to the neuronal *rab*-Gal4 lines, Rabs that exhibit both synaptic and cell body localization are not

motorneurons or because these more restrictively expressed *rabs* are not expressed in motorneurons (Figure S6A).

Several Rabs mark large, distinct subcellular compartments, whereas others exhibit more diffuse localization. To assess the molecular nature of the compartments marked by Rab proteins in the neurons where they are endogenously expressed, we colabeled YFP-Rabs driven by their corresponding *rab*-Gal4 lines with antibodies against early (Rab5), late (Rab7), and recycling endosome (Rab11) markers and the synaptic vesicle marker cysteine-string protein (CSP). Seven Rabs exhibit strong colocalization with large, distinct Rab11-positive recycling endosomes specifically at synapses. Interestingly, six of these seven are neuronal Rabs (Rab19, Rab21, Rab26, Rab32, RabX1, and RabX4) (Table 1). We

(red), and Toto-3 labels nuclei (blue). The top left corner shows an anterior brain schematic with the lamina (red) and the mushroom bodies and antennal lobes (green) and a posterior brain schematic showing the cell bodies of the Kenyon cells that form the mushroom body (green) and the optic neuropils medulla and lobula complex (red). Glia is marked in yellow. The different *rab*-Gal4 lines drive expression in these structures with highly varying intensity. Scale bar for all panels represents 100 μ m.

Table 1. Subcellular Localization Profiling Summary

	Cellular	Coloc./Compartment	Subcellular Localization			Compartment Identity		
			WT	CA	DN	WT	CA	DN
Rab3	N	CSP (strong)	S	S	diffuse	diffuse	diffuse	diffuse
RabX4	N	Rab11 (strong aggregation phenotype)	S	S	diffuse	strong	mix	diffuse
Rab27	N	CSP (strong)	S	S	?	diffuse	diffuse	?
Rab26	N	Rab11 (strong aggregation phenotype)	S	S	diffuse	strong	strong	diffuse
Rab19	N	Rab11 (aggregation phenotype)	Se	Se	diffuse	strong	unclear	diffuse
Rab32	N	Rab11 (aggregation phenotype)	Se	S	Se	strong	strong	diffuse
RabX1	N	Rab11 (strong aggregation phenotype)	S	S	?	strong	strong	?
Rab23	SNE	Rab11 (aggregation phenotype)	Se	Se	diffuse	mix	mix	diffuse
Rab21	SNE	Rab11 (mild aggregation phenotype)	S	Se	diffuse	strong	diffuse	diffuse
Rab9	SNE	some CSP&Rab11	S	S	diffuse	mix	mix	weak
Rab4	NE	-	Se	S	diffuse	strong	strong	diffuse
Rab7	NE	Rab7 (strong)	mix	mix	diffuse	strong	strong	weak
Rab14	maybe Ubi?	Rab7 (strong)	mix	Se	?	strong	diffuse	?
Rab10	maybe Ubi?	Rab11 (strong aggregation phenotype)	mix	mix	S	weak	diffuse	strong
Rab39	Ubi	Rab7	mix	mix	diffuse	strong	diffuse	diffuse
Rab18	maybe Ubi?	Rab5 (changes Rab5 localization)	cb	?	diffuse	diffuse	?	diffuse
Rab8	Ubi	some CSP&Rab11 (some Rab11 aggregation)	Se	diffuse	diffuse	weak	diffuse	diffuse
Rab2	Ubi	-	mix	Se	diffuse	weak	weak	diffuse
Rab1	Ubi	-	cb	mix	lethal	strong	diffuse	lethal
Rab6	Ubi	-	Se	Se	diffuse	weak	weak	diffuse
Rab35	Ubi	-	mix	Se	diffuse	diffuse	diffuse	diffuse
Rab5	Ubi	Rab5 (strong)	mix	mix	lethal	strong	strong	lethal
Rab11	Ubi	Rab11 (very strong aggregation phenotype)	mix	diffuse	lethal	strong	diffuse	lethal

The following abbreviations are used: WT, wild-type; CA, constitutively active; DN, dominant negative; N, neuron-specific; SNE, strongly neuron-enriched; NE, neuron-enriched; Ubi, ubiquitous; S, synaptic; Se, synapse-enriched; cb, cell body; mix, cell body and synapses (abbreviations used in the Subcellular Localization column and distinct and diffuse labeling in the Compartment Identity column). “?” indicates the YFP signal was too weak. “Compartment Identity” refers to how distinct YFP punctae appears.

further observed that expression of all seven Rab11-positive YFP-Rabs caused larger Rab11-positive compartments than observed in the Rab11 immunolabeling expressing other YFP-Rabs (Figure S5B). This suggests that the overexpression of these Rabs causes an increase in types of recycling endosomal compartments at synapses. Only Rab3 and Rab27 exhibit strong colocalization with the synaptic vesicle marker CSP. YFP-Rab8 and YFP-Rab9 exhibit partial colocalization with both CSP and Rab11. YFP-Rab14 and YFP-Rab39 exhibit significant colocalization with the late endosomal marker Rab7. YFP-Rab18 is the only Rab protein (other than YFP-Rab5) that exhibits strong colocalization with anti-Rab5 labeling and also clearly changes Rab5 localization. Finally, five YFP-Rabs (Rab1, Rab2, Rab4, Rab6, Rab35) exhibit no significant colocalization with any of the four immunolabels (Figure S5A; Table 1). The subcellular localization profiling of wild-type Rabs thus reveals that the majority of novel neuronal rabs encode synaptic proteins that mark Rab11-positive synaptic recycling endosomal compartments.

Expression of Constitutively Active and Dominant-Negative Rab GTPases in Their Endogenous Expression Patterns

Functional analyses of *rab* GTPases can be performed using the GTP bound (constitutively active, CA) or GDP bound (dominant negative, DN) mutants [16]. We performed a functional profiling of all Rab proteins analyzed here by investigating the CA and DN variants expressed in their endogenous expression patterns (Figure 5). Remarkably, only the DN variants of the ubiquitous Rab1, Rab5, Rab11, and Rab35 cause lethality. None of the CA or DN variants of the neuronal Rabs caused obvious developmental or functional defects. We also tested dominant-negative expression for the nine most neuronal Rabs at the neuromuscular junction and did not

observe any obvious morphological defects (Figures S6A and S6B). These data suggest that neuronal *rabs* may serve modulating or partially redundant functions. This idea is consistent with the findings that a mutant of the best characterized panneuronal *rab3* is viable in *Drosophila* [15], and a quadruple knockout for all four vertebrate *rab3* isoforms in mice develops normally, is born alive, and has a surprisingly mild defect on neuronal function [26]. In addition, the functional profiling of CA and DN Rabs revealed that the neuronal Rabs that mark synaptic Rab11-positive compartments (RabX4, Rab26, Rab19, Rab32, RabX1, Rab21) again show a common behavior: both the wild-type (WT) and CA variants mark distinct compartments at synapses, whereas the DN variants exhibit no preferential synaptic localization and are diffusely distributed throughout the neurons (Figure 5). This is in accordance with the observation that GTP-bound Rabs exhibit increased labeling of specific compartments. Similarly, the well-characterized endosomal marker proteins Rab5 and Rab7 label increased endosomal compartments as CA variants (Figure 5). A notable exception is Rab10, which exhibits increased synaptic aggregations when the dominant-negative version is expressed and a more diffuse neuronal labeling when the constitutively active form is expressed. Among the ubiquitous Rabs, Rab2 shows the most neuronal subcellular relocalization behavior, i.e., synaptic enrichment of Rab2CA and loss of localization for Rab2DN. Taken together, our findings suggest that synapses are the principle site of action for neuronal Rabs based on RabCA protein localization.

Generation of a *rab27* Knockout by Ends-Out Homologous Recombination of the Gal4 Knockin Cassette Reveals a Specific Sleep Phenotype

The objective of our profiling effort was to identify synaptic Rabs that potentially play roles in brain development and

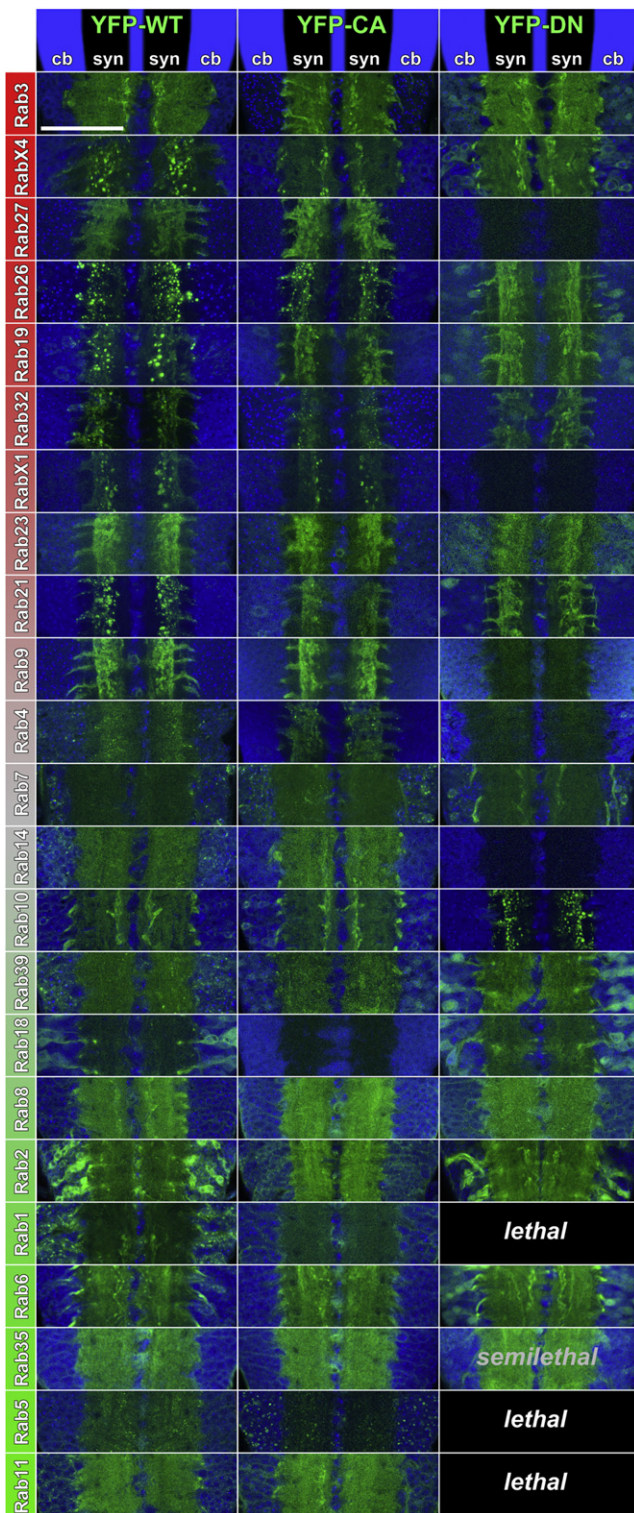


Figure 5. Subcellular Localization Profiling as a Function of GTP- and GDP-Bound States

Proximal ventral ganglion sections are shown sorted for all Rabs from most neuronal (top, red) to most ubiquitously expressed (bottom, green), similar to Figure 4. Corresponding Gal4-lines drive the expression of wild-type YFP-tagged Rabs in the left column, constitutively active (GTP-bound) YFP-tagged Rabs in the middle column, and dominant-negative (GDP-bound) YFP-tagged Rabs in the right column. Toto-3 labels nuclei (blue). Note that most neuronal Rabs show synaptic localization and little or no

function and at the same time provide the tools to generate knockouts in these genes. Our Gal4 knockin cassettes can be mobilized in vivo and targeted to endogenous loci using ends-out homologous recombination [20] (Figure S6). This technique is, to our knowledge, the first application of BAC recombineering to utilize genomic fragments as large (10–20 kb) homology arms in *Drosophila* gene targeting. Furthermore, our strategy differs from published techniques in that the targeting cassette is positively marked with 3xP3-RFP and can be separated from the differently marked landing site (yellow +) and P[acman] backbone (white +) (Figure S6; Supplemental Experimental Procedures).

We chose *rab27* for a “proof-of-principle” knockout screen for two reasons: first, it is the only strong synaptic vesicle marker other than the well-characterized *rab3*, consistent with a recent characterization of its role in synaptic vesicle exocytosis [27]; second, *rab27* exhibits a highly specific expression pattern in brain structures with known functions. We screened approximately 30,000 F2 progeny for separation of the targeting cassette from the mobilization site and identified 37 reintegrations of the targeting cassette away from the mobilization site. Thirty-two of the 37 genomic integration events occurred on the X chromosome, where the endogenous *rab27* gene maps. Twenty-four of the 32 lines were subsequently tested by PCR (12 shown in Figure 6A), indicating that the *rab27* open reading frame was correctly replaced with the Gal4 cassette in six lines. The resulting recombination frequency is 1 in 4,000 or 2.5×10^{-4} , which is higher than the homologous recombination efficiency reported in a comparable recent report [28]. Finally, we tested and confirmed two lines by Southern blotting with a DNA probe against the *rab27* open reading frame (Figure 6B). UAS-YFP-Rab27 driven by *rab27*-Gal4 in the landing site (Figures 6C and 6E) or *rab27*-Gal4 knocked into the endogenous locus (Figures 6D and 6F) exhibit identical Rab27 expression, corroborating that the 40 kb genomic targeting cassette likely contained all the functionally significant regulatory elements of the endogenous locus.

rab27 homozygous mutant adults are viable and fertile. Previous results demonstrated that mushroom bodies, which exhibit specific expression of *rab27*, regulate sleep in flies [29, 30]. To determine whether loss of *rab27* causes a behavioral phenotype, we assayed activity, circadian rhythm, and sleep behavior of *rab27^{Gal4-KO}*. *rab27^{Gal4-KO}* flies displayed normal activity levels and rhythm strength in a 12 hr/12 hr light/dark (LD) cycle (Figures S7A–S7C). Measurements of the duration of the longest sleep bout for each day and night, showed a significant reduction during the daytime for *rab27^{Gal4-KO}*. Analysis of all bouts revealed a more than 30% reduction in median and top quartile bout length for *rab27^{Gal4-KO}* homozygotes compared to controls in the same *yw* genetic background (Figures 6G–6J). This phenotype can be rescued by expressing UAS-YFP-*rab27* driven by *rab27^{Gal4-KO}* (Figure 6H). Hence, loss of *rab27* leads to less consolidated daytime sleep, consistent with its cell-specific expression in mushroom bodies. This cell specificity is preserved for two isoforms of *rab27*, both of which are

cell body localization that is maintained and further enriched as constitutively active but lost as dominant-negative versions. Further note that only expression of the dominant negatives of Rab1, Rab5, and Rab11 cause embryonic or early larval lethality, whereas Rab35 dominant negative is semilethal with few adult escapers. A high-resolution version of this figure is available online. Scale bar for all panels represents 50 μ m.

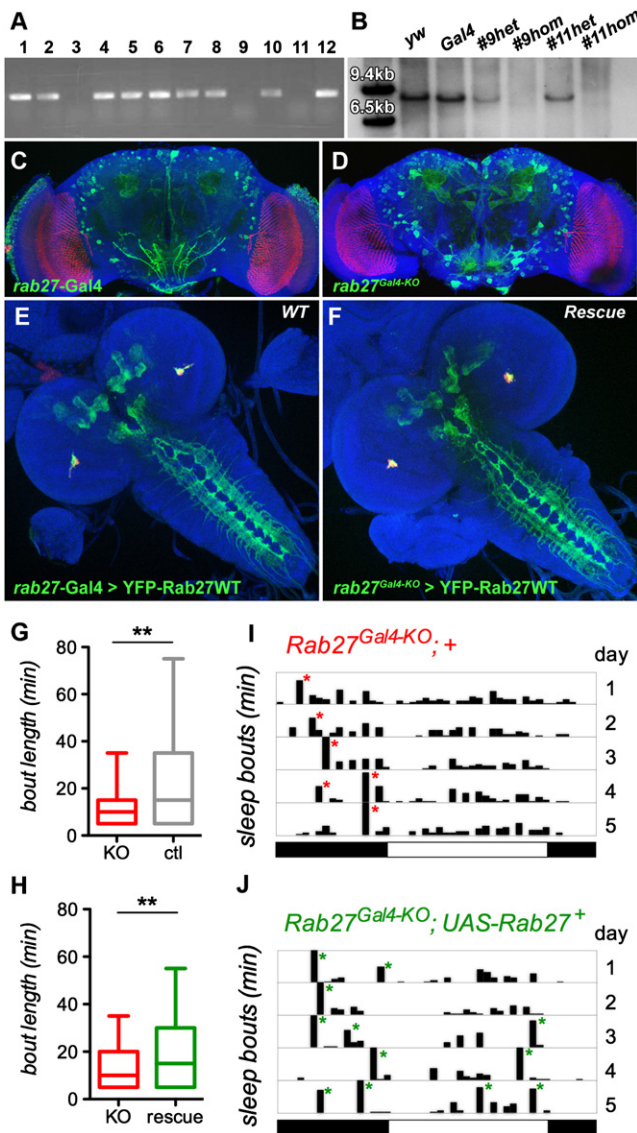


Figure 6. Generation of a *rab27* Knockout by Ends-Out Homologous Recombination of the Gal4 Knockin Cassette Reveals a Specific Sleep Phenotype

(A) PCR verification of 3xP3-RFP positive targeting cassette mobilizations and reintegrations in the genome indicate loss of the endogenous *rab27* locus for three out of 12 potential knockout lines.

(B) Verification of two of the knockouts by Southern blot with an ORF probe (see Figure S6).

(C and D) *rab27*-Gal4 in the landing site and *rab27^{Gal4-KO}* in the endogenous site exhibit very similar expression patterns (CD8-GFP in green) specific to the mushroom bodies in the adult brain.

(E and F) YFP-tagged Rab27 expression is identical between YFP-Rab27 in wild-type using *rab27*-Gal4 and YFP-Rab27 rescuing expression in a homozygous null mutant with *rab27^{Gal4-KO}* knockin.

(G and H) Sleep phenotype in *rab27^{Gal4-KO}* flies. *rab27^{Gal4-KO}* flies show decreased daytime sleep bout length (median, quartiles, 90th percentile) compared to controls (G), a phenotype rescued by introducing the *UAS-Rab27-YFP* transgene (H).

(I and J) Representative single fly sleepograms showing decreased bout length. Each bar represents a sleep bout, with the height indicating the duration (y axis = 120 min, x axis = 24 hr, light/dark cycle indicated by white/black boxes). *rab27^{Gal4-KO}* flies have a decreased number of long, >60 min sleep bouts (indicated by asterisk), especially during the daytime, compared to *rab27^{Gal4-KO}; UAS-rab27-YFP* rescue flies.

knocked out in *rab27^{Gal4-KO}* (Figures S7D–S7F). Our data suggest that the cell-specific expression of neuronal *rabs* in different parts of the brain may relate to surprisingly specialized functions.

Discussion

In this paper, we present a novel approach to functional profiling of gene families in *Drosophila* by combining BAC recombineering with ends-out homologous recombination. We used this approach to generate 36 transgenic *rab*-Gal4 lines and performed systematic cellular and subcellular expression profiling of 23 Rab proteins. We report the surprising findings that (1) half of all Rabs are neuronal-specific or neuron-enriched, (2) different neuronal Rabs function in distinct subsets of neurons in the brain, (3) all neuronal Rabs localize to synapses, and (4) synaptic Rabs predominantly recruit and mark Rab11-positive synaptic recycling endosomal compartments. Finally, we demonstrate the mobilization and homologous recombination of the Gal4 knockin cassette by generating a knockout for the neuron-specific *rab27* gene. This *rab27^{Gal4-KO}* null mutant exhibits a specific behavioral sleep phenotype that matches the cell-specific expression pattern.

An Improved Transgenesis Platform for *Drosophila*

Homologous recombination techniques in *Drosophila* have hitherto been limited by difficult vector construction and inefficient in vivo recombination. BAC recombineering allows streamlined cloning independent of restriction enzymes or other sequence-specific restrictions. We modified the existing BAC recombineering-based P[acman] vector [31] by incorporating a cassette for ends-out homologous recombination [20]. The underlying idea is to utilize large genomic fragments as homology arms for gene targeting instead of conventional PCR-based and size-restricted homology arms. We find that the key advantage of this technique lies in the ease of base-pair precise manipulation of genomic fragments in a single round of recombineering once the parent vector with genomic region has been generated. This is demonstrated in this paper for numerous alternative Gal4 knockins for the various *rab* loci. In contrast, PCR-based cloning often requires complete redesign for each targeting vector. The ability to systematically characterize cellular and subcellular expression patterns prior to performing an ends-out homologous recombination screen represents a second key strategic advantage for the present study. The large genomic fragments are several times larger than traditional genomic rescue constructs in *Drosophila*, thereby ensuring the expression accuracy of the Gal4 knockins. We chose Gal4 knockins as highly versatile tools, especially in light of the earlier generation of a complete collection of UAS-YFP-tagged *rab* strains [16]. Gal4 knockins thus provide means for subcellular profiling and rescue using YFP-tagged proteins expressed under their own regulatory elements. In summary, the vectors and protocols generated here may provide a widely applicable method to modify large genomic constructs that can be mobilized for homologous recombination in a separate experimental step.

Our mobilization of the 40 kb *rab27* Gal4 targeting cassette by standard heat shock activation of the flippase (FLP) and ISce1 enzymes was efficient. In contrast to previous implementations of ends-out homologous recombination in *Drosophila*, our knockin cassette is positively marked with

eye-specific RFP expression, thereby providing a simple means to follow the separation of the targeting cassette from the landing site and reintegration somewhere else in the genome with a rate of 1 in ~ 800 progeny. More than 85% of the reintegration events were on the correct target chromosome, and 25% of these correct target chromosome insertions were correct gene replacements. This brings the final recombination frequency to 1 in 4,000 or 2.5×10^{-4} , which compares favorably to rates between 7×10^{-6} and 1.9×10^{-4} in a recent report on improved ends-out homologous recombination for six different loci [28]. Because homologous recombination is highly locus-specific, it is too early to quantitatively assess our method. In particular, a systematic test of the effect of homology arm length on recombination frequency has not been performed in *Drosophila*. P[acman]-KO may provide an effective means to test and implement further improvements of almost restriction-free genomic gene manipulation in *Drosophila* on a medium to large scale.

Novel Insights into Rab Function in the Nervous System

The development of a BAC recombineering-based gene targeting technique was motivated by the desire to systematically study a large gene family in vivo. *rab* GTPases have been at the focal point of several systematic profiling efforts and dubbed the “membrome” as a result of their common and yet diversified functional significance for all intracellular membrane trafficking [32]. Many aspects of the earlier microarray-based expression profiling are consistent with our finding, e.g., the neuronal expression of *rab3* and *rab26*. However, a previous microarray-based profiling study did not observe the overall bias toward nervous system expression [32]. For example, both vertebrate *rab27* isoforms were found to be expressed at low levels in the brain, yet we identify *rab27* as a neuron-specific *rab* with highly restricted expression in the brain. Such cell-type-specific expression is likely obscured in any microarray study, which by necessity assays a heterogeneous population of cells. Importantly, a partially overlapping role of the molecular functions of *rab27* and *rab3* was recently described for synaptic neurotransmitter release [27]. Although this finding is consistent with our identification of *rab27* and *rab3* as the strongest synaptic vesicle colocalizing *rabs*, the restricted *rab27* expression pattern makes it an unlikely general regulator of exocytosis in *Drosophila*. We surmise that the cellular and subcellular resolution profiling presented here captures important information about Rab protein localization that was not attainable in earlier studies on homogenized tissues.

Our functional profiling with wild-type, constitutively active, and dominant-negative Rabs expressed in their endogenous expression patterns suggest that few, if any, of the neuronal *rab* GTPases are required for neuronal viability. One possible explanation is that dominant-negative Rab expression may be a poor substitute for genetic loss-of-function alleles. An alternative or additional explanation may be partially redundant functions, which can be investigated with the tools presented here. Indeed, the best characterized neuronal *rab3* is viable in *Drosophila* [15]. Similarly, a quadruple knockout for all four vertebrate *rab3* isoforms in mice develops normally, is born alive, and has a surprisingly mild defect on neuronal function [26]. In addition, we show here that a null mutant for the second synaptic vesicle-associated Rab, *rab27*, is viable. Interestingly, both loss of *rab3* and loss of *rab27* cause mild and specific neuronal phenotypes [15, 26]. Taken together,

these data lead us to speculate that neuronal *rabs* may serve specialized, modulatory functions in neurons.

Our subcellular localization profiling revealed that all neuronal Rab proteins (Rab3, RabX4, Rab27, Rab26, Rab19, Rab23, Rab32, RabX1, Rab21, Rab9) localize highly preferentially or exclusively to synapses. This observation suggests that the specialized or modulatory functions of neuronal *rabs* serve specific demands on membrane trafficking at synapses. This observation may not be too surprising, given that the axon termini are arguably the most specialized and distinct cellular compartments of neurons in comparison with other cell types. However, the identification of six of these ten neuronal and synaptic Rab proteins as markers of Rab11-positive compartments is remarkable. Rab11 is a “gold-standard” marker for recycling endosomal compartments [33]. The highly regulated recycling of transmitter release machinery, AMPA receptors, and guidance receptors, to name but a few, may provide an explanation for the existence of such extensive, specialized synaptic membrane trafficking machinery. In this paper, we provide the tools and techniques to dissect this machinery in vivo.

Experimental Procedures

Drosophila Strains and Genetics

For all *rab*-Gal4 transgenic strains, we used the landing site attP-3B (Bloomington Stock #24871). The following mutant chromosomes for rescue experiments were obtained: *rab3^{rup}* (gift from Aaron DiAntonio); *rab6^{ASI}*, *Frt40A* (gift from Spyros Artavanis-Tsakonis); *rab6[D23D]*, *Frt40A* (gift from Hugo Bellen); and stocks #8907 and #25729 from the Bloomington Stock Center. Rescue experiments were set up as follows: Rab3: Df(2R)BSC639/CyO; UAS-YFP-Rab3-WT/TM3 X *rab3^{rup}*/CyO; *rab3*-ATG-Gal4/TM3. Rab6: *rab6[D23D]*, UAS-YFP-Rab6-WT/CyO X Df(2L)ED775/CyO; *rab6*-Gal4/TM3. Rab6: *rab6^{ASI}*, *FRT40A*/CyO; UAS-YFP-Rab6-WT/TM3 X *rab6^{ASI}*, *FRT40A*/CyO; *rab6*-Gal4/TM3. See Supplemental Experimental Procedures for full description of genetics and genotypes used.

Molecular Biology and Recombineering

attB-P[acman]-KO was generated by inserting FRT/I-Sce1 site into the existing Pac1 and Asc1 sites of attB-P[acman] [31] such that the original Pac1 and Asc1 sites were destroyed and new Asc1 and Pac1 sites generated proximally (Figure 1). Second, the Gateway™ BP recombination cassette from pDONR221 was inserted to facilitate cloning proximally of the FRT/I-Sce1 sites independent of the Asc1 and Pac1 sites. The Gal4 knockin cassette is described in detail in the Supplemental Experimental Procedures. The recombineering protocol was adapted from [31] with the following modifications: for first round recombineering, two 500 bp homology arms (left arm [LA] and right arm [RA]) flanking the 40 kb fragment were PCR soe'd, with a BamH1 site added in the middle and attB1 and attB2 site at the ends. The 1 kb PCR products were cloned into P[acman]-KO using the Gateway BP reaction following manufacturer's instruction (Invitrogen BP clonase II 11789-020). Ten micrograms of the resulting P[acman]-KO-1kb was digested with BamH1-HF (New England Biolabs [NEB] R3136S) at 37°C for 6 hr. After gel electrophoresis, DNA was extracted with Zymoclean Gel DNA recovery kit (Zymoresearch D4008). Five microliters of total 12 μ l DNA eluate was electroporated into recombineering-competent DY380 cells. To verify the colonies, we verified both LA and RA junctions by PCR using primers outside of the 500 bp regions and then sequenced. Second round recombineering involved two 100 bp sequences flanking the target region that were added to the Gal4-RFP-Kan cassette as homology arms by PCR using Phusion® High-Fidelity DNA Polymerase (Finnzymes, Cat # F-530S) kit with the following conditions and cycling: sterile water 35.5 μ L, 5 \times Phusion HF Buffer 10 μ L, MgCl₂ (50 mM) 1 μ L, dNTPs (10 mM TOTAL) 1.5 μ L, forward primer (10 uM) 0.5 μ L, reverse primer (10 uM) 0.5 μ L, p-ENTR-Gal4 (45 ng/ μ L) 0.5 μ L, Phusion DNA polymerase 0.5 μ L. After gel electrophoresis, a 6.7 kb band was excised and extracted with the Zymoclean kit. One hundred nanograms of DNA was transformed into recombineering-competent DY380 cells containing P[acman]-KO-40 kb. The transformants were selected from Tet-Amp-Kan triple selective LB plates, and colonies were verified by PCR and confirmed by sequencing

[P[acman]-Gal4). DNA from confirmed colonies was extracted and transformed into EPI300 cells for copy number induction and subsequent injection (Rainbow Transgenics). We note that the preparation of high quality DNA proved a key requirement for all steps from recombineering to transgenesis. The detailed recombineering protocol is available in [Supplemental Experimental Procedures](#).

Immunohistochemistry, Microscopy, and Image Processing

Adult brains, eyes, and eye-lamina complexes as well as pupal brains and eye-brain complexes were dissected as reported [34]. The tissues were fixed in phosphate buffered saline (PBS) with 3.5% formaldehyde for 15 min and washed in PBS with 0.4% Triton X-100. High-resolution light microscopy was performed using the Resonance Scanning Confocal Microscope Leica SP5. Imaging data was processed and quantified using Amira 5.2 (Indeed) and Adobe Photoshop CS4 as described in [35]. The following antibodies were used at 1:500: rabbit anti-rab5, rabbit anti-rab7, mouse anti-rab11. A mouse monoclonal antibody against CSP was used at 1:50.

Knockout Screen

A full crossing scheme is depicted in [Figure S6](#). In brief, *rab27*-Gal4 male transformants containing the Gal4 cassette in the landing site were crossed to females with *hs-FLP* and *hs-I-SceI* (Bloomington stock number 6935). Forty-eight hours after egg laying, embryos were heat-shocked at 37°C (twice per day for 3 consecutive days). Twenty-four of 32 lines were subsequently verified by PCR for both 3' and 5' junctions of the open reading frame. Six of 24 are negative in PCR, indicating the replacement of *rab27* open reading frame with the cassette. The primers for PCR are listed below: 5' junction fwd, 5-TCGCAGATTCCTCCAGATC-3; 5' junction rev, 5-CAATTA GGAGCAAACCAACAA-3; 3' junction fwd, 5-ATGGGTTTCCTGCTCATCTT-3; 3' junction rev, 5-GCAGGCATCGCGACTGGGTC-3.

Southern Blot

Genomic DNA was prepared following Quick Fly Genomic DNA Prep from the Berkeley Drosophila Genome Project (<http://www.fruitfly.org/about/methods/inverse.pcr.html>). Twenty micrograms of DNA from each strain were digested with *NheI*-HF (NEB R3131S, 25 U) at 37°C for overnight, and then separated using 4% DNA gel at 35 V, 4°C for overnight. The gel was subsequently incubated in Denaturing solution (1.5 M NaCl, 0.5 M NaOH) for 45 min, Depurination solution (0.2 N HCl) for 15 min, Neutralization solution (1 M Tris pH 7.4, 1.5 M NaCl) twice for 30 min, and then transferred onto a membrane (Amersham Hybond-N RPN303N) using 10% saline-sodium citrate (SSC) buffer at room temperature for overnight. The membrane was crosslinked by UV and incubated in preheated hybridization buffer (Roche 11796895001) for 30 min at 42°C. Dig-labeled *Rab27* ORF probe was generated by PCR using the following primers: 5'-TTGACG TTGGCGCCGGTGCA-3', 5'-TGAGCCTCTGCAATTAGCCGGAT-3', labeled with Dig using Klenow (NEB) with labeling mix (NEB), boiled for 5 min to denature, and added to the membrane for hybridization overnight at 45°C. At room temperature, the membrane was washed twice in 2× SSC, 0.1% SDS for 20 min each, twice in 0.5× SSC, 0.1% SDS at 68°C for 30 min each, rinsed in maleic acid buffer (100 mM maleic acid, 150 mM NaCl, pH 7.5) with shaking for 5 min, blocked in block reagent (Roche 11096176001) for 3 hr, incubated in block solution with anti-Dig antibody (1:1,000, 11093274910) for 30 min, washed twice in wash buffer (30 ml maleic acid buffer with 90 μl Tween 20) for 15 min each, rinsed in detection buffer (0.1 M Tris, 0.1 M NaCl pH 9.5) for 5 min, immersed in CDP-Star solution, and then exposed to film for visualization.

Behavioral Analysis

Flies were assayed in a *yw* genetic background, and experimental and controls always were in identical, though sometimes hybrid, backgrounds. Flies were entrained for 3 days and assayed in a 12hr/12hr light/dark incubator and monitored with the *Drosophila* Activity Monitor system (TriKinetics). Sleep times were determined as described [30].

Supplemental Information

Supplemental Information includes seven figures and Supplemental Experimental Procedures and can be found with this article online at [doi:10.1016/j.cub.2011.08.058](https://doi.org/10.1016/j.cub.2011.08.058).

Acknowledgments

We would like to thank Matthew Scott, Hugo Bellen, Aaron DiAntonio, Spyros-Artavanis-Tsakonas, Patrick Dolph, the Bloomington Stock Center,

and the University of Iowa Developmental Studies Hybridoma Bank for reagents. We further thank Koen Venken, Hugo Bellen, Nevine Shalaby, Tong-Wey Koh, and all members of the Buszczak and Hiesinger laboratories for discussion and comments on the manuscript. We are especially grateful to Susanne Eaton for discussion and communication of results prior to publication and to Nevine Shalaby for help with Southern blotting. Technical assistance by Elzi Volk in the early stages of this project and by Ossama Saladin during revision is gratefully acknowledged. This work was supported by grants from the National Institutes of Health to P.R.H. (R01EY018884), M.B. (R01GM086647), and A.R. (R01AA019526); a visual sciences core grant (EY020799); a grant by the Cancer Prevention Research Institute of Texas to M.B. and P.R.H. (RP100516); and the Whitehall Foundation and the Welch Foundation (I-1657) to P.R.H. A.R. is an Effie Marie Cain Scholar in Biomedical Research, M.B. is an E.E. and Greer Garson Fogelson Scholar in Biomedical Research, and P.R. Hiesinger is a Eugene McDermott Scholar in Biomedical Research at UT Southwestern Medical Center.

Received: July 4, 2011

Revised: August 18, 2011

Accepted: August 26, 2011

Published online: October 13, 2011

References

1. Touchot, N., Chardin, P., and Tavitian, A. (1987). Four additional members of the ras gene superfamily isolated by an oligonucleotide strategy: molecular cloning of YPT-related cDNAs from a rat brain library. *Proc. Natl. Acad. Sci. USA* **84**, 8210–8214.
2. Zerial, M., and McBride, H. (2001). Rab proteins as membrane organizers. *Nat. Rev. Mol. Cell Biol.* **2**, 107–117.
3. Pfeffer, S.R. (2007). Unsolved mysteries in membrane traffic. *Annu. Rev. Biochem.* **76**, 629–645.
4. Pfeffer, S.R. (1994). Rab GTPases: master regulators of membrane trafficking. *Curr. Opin. Cell Biol.* **6**, 522–526.
5. Stenmark, H. (2009). Rab GTPases as coordinators of vesicle traffic. *Nat. Rev. Mol. Cell Biol.* **10**, 513–525.
6. Molendijk, A.J., Ruperti, B., and Palme, K. (2004). Small GTPases in vesicle trafficking. *Curr. Opin. Plant Biol.* **7**, 694–700.
7. Pfeffer, S., and Aivazian, D. (2004). Targeting Rab GTPases to distinct membrane compartments. *Nat. Rev. Mol. Cell Biol.* **5**, 886–896.
8. Aligianis, I.A., Johnson, C.A., Gissen, P., Chen, D., Hampshire, D., Hoffmann, K., Maina, E.N., Morgan, N.V., Tee, L., Morton, J., et al. (2005). Mutations of the catalytic subunit of RAB3GAP cause Warburg Micro syndrome. *Nat. Genet.* **37**, 221–223.
9. Ménasché, G., Pastural, E., Feldmann, J., Certain, S., Ersoy, F., Dupuis, S., Wulffraat, N., Bianchi, D., Fischer, A., Le Deist, F., and de Saint Basile, G. (2000). Mutations in RAB27A cause Griscelli syndrome associated with haemophagocytic syndrome. *Nat. Genet.* **25**, 173–176.
10. Verhoeven, K., De Jonghe, P., Coen, K., Verpoorten, N., Auer-Grumbach, M., Kwon, J.M., FitzPatrick, D., Schmedding, E., De Vriendt, E., Jacobs, A., et al. (2003). Mutations in the small GTP-ase late endosomal protein RAB7 cause Charcot-Marie-Tooth type 2B neuropathy. *Am. J. Hum. Genet.* **72**, 722–727.
11. Mitra, S., Cheng, K.W., and Mills, G.B. (2011). Rab GTPases implicated in inherited and acquired disorders. *Semin. Cell Dev. Biol.* **22**, 57–68.
12. Nachury, M.V., Loktev, A.V., Zhang, Q., Westlake, C.J., Peränen, J., Merdes, A., Slusarski, D.C., Scheller, R.H., Bazan, J.F., Sheffield, V.C., and Jackson, P.K. (2007). A core complex of BBS proteins cooperates with the GTPase Rab8 to promote ciliary membrane biogenesis. *Cell* **129**, 1201–1213.
13. Satoh, A.K., O'Tousa, J.E., Ozaki, K., and Ready, D.F. (2005). Rab11 mediates post-Golgi trafficking of rhodopsin to the photosensitive apical membrane of *Drosophila* photoreceptors. *Development* **132**, 1487–1497.
14. Mehta, S.Q., Hiesinger, P.R., Beronja, S., Zhai, R.G., Schulze, K.L., Verstreken, P., Cao, Y., Zhou, Y., Tepass, U., Crair, M.C., and Bellen, H.J. (2005). Mutations in *Drosophila* *sec15* reveal a function in neuronal targeting for a subset of exocyst components. *Neuron* **46**, 219–232.
15. Graf, E.R., Daniels, R.W., Burgess, R.W., Schwarz, T.L., and DiAntonio, A. (2009). Rab3 dynamically controls protein composition at active zones. *Neuron* **64**, 663–677.
16. Zhang, J., Schulze, K.L., Hiesinger, P.R., Suyama, K., Wang, S., Fish, M., Acar, M., Hoskins, R.A., Bellen, H.J., and Scott, M.P. (2007). Thirty-one flavors of *Drosophila* rab proteins. *Genetics* **176**, 1307–1322.

17. Ali, B.R., and Seabra, M.C. (2005). Targeting of Rab GTPases to cellular membranes. *Biochem. Soc. Trans.* 33, 652–656.
18. Jordens, I., Marsman, M., Kuijl, C., and Neefjes, J. (2005). Rab proteins, connecting transport and vesicle fusion. *Traffic* 6, 1070–1077.
19. Venken, K.J., and Bellen, H.J. (2007). Transgenesis upgrades for *Drosophila melanogaster*. *Development* 134, 3571–3584.
20. Gong, W.J., and Golic, K.G. (2003). Ends-out, or replacement, gene targeting in *Drosophila*. *Proc. Natl. Acad. Sci. USA* 100, 2556–2561.
21. Sharan, S.K., Thomason, L.C., Kuznetsov, S.G., and Court, D.L. (2009). Recombineering: a homologous recombination-based method of genetic engineering. *Nat. Protoc.* 4, 206–223.
22. Venken, K.J., Popodi, E., Holtzman, S.L., Schulze, K.L., Park, S., Carlson, J.W., Hoskins, R.A., Bellen, H.J., and Kaufman, T.C. (2010). A molecularly defined duplication set for the X chromosome of *Drosophila melanogaster*. *Genetics* 186, 1111–1125.
23. Venken, K.J., Carlson, J.W., Schulze, K.L., Pan, H., He, Y., Spokony, R., Wan, K.H., Koriabine, M., de Jong, P.J., White, K.P., et al. (2009). Versatile P[acman] BAC libraries for transgenesis studies in *Drosophila melanogaster*. *Nat. Methods* 6, 431–434.
24. Freeman, M. (1996). Reiterative use of the EGF receptor triggers differentiation of all cell types in the *Drosophila* eye. *Cell* 87, 651–660.
25. Zerial, M. (1993). Regulation of endocytosis by the small GTP-ase rab5. *Cytotechnology* 11 (Suppl 1), S47–S49.
26. Schlüter, O.M., Schmitz, F., Jahn, R., Rosenmund, C., and Südhof, T.C. (2004). A complete genetic analysis of neuronal Rab3 function. *J. Neurosci.* 24, 6629–6637.
27. Pavlos, N.J., Grønberg, M., Riedel, D., Chua, J.J., Boyken, J., Kloepper, T.H., Urlaub, H., Rizzoli, S.O., and Jahn, R. (2010). Quantitative analysis of synaptic vesicle Rabs uncovers distinct yet overlapping roles for Rab3a and Rab27b in Ca²⁺-triggered exocytosis. *J. Neurosci.* 30, 13441–13453.
28. Huang, J., Zhou, W., Dong, W., Watson, A.M., and Hong, Y. (2009). From the Cover: Directed, efficient, and versatile modifications of the *Drosophila* genome by genomic engineering. *Proc. Natl. Acad. Sci. USA* 106, 8284–8289.
29. Joiner, W.J., Crocker, A., White, B.H., and Sehgal, A. (2006). Sleep in *Drosophila* is regulated by adult mushroom bodies. *Nature* 441, 757–760.
30. Pitman, J.L., McGill, J.J., Keegan, K.P., and Allada, R. (2006). A dynamic role for the mushroom bodies in promoting sleep in *Drosophila*. *Nature* 441, 753–756.
31. Venken, K.J., He, Y., Hoskins, R.A., and Bellen, H.J. (2006). P[acman]: a BAC transgenic platform for targeted insertion of large DNA fragments in *D. melanogaster*. *Science* 314, 1747–1751.
32. Gurkan, C., Lapp, H., Alory, C., Su, A.I., Hogenesch, J.B., and Balch, W.E. (2005). Large-scale profiling of Rab GTPase trafficking networks: the membrome. *Mol. Biol. Cell* 16, 3847–3864.
33. Ullrich, O., Reinsch, S., Urbé, S., Zerial, M., and Parton, R.G. (1996). Rab11 regulates recycling through the pericentriolar recycling endosome. *J. Cell Biol.* 135, 913–924.
34. Williamson, W.R., and Hiesinger, P.R. (2010). Preparation of developing and adult *Drosophila* brains and retinae for live imaging. *J. Vis. Exp.* 15, 1936.
35. Williamson, W.R., Yang, T., Terman, J.R., and Hiesinger, P.R. (2010). Guidance receptor degradation is required for neuronal connectivity in the *Drosophila* nervous system. *PLoS Biol.* 8, e1000553.